

# Magnetic and electronic properties of substitutional $\text{Fe}_N$ cluster impurities in Cr: Transition from antiferromagnetic to ferromagnetic $\text{Fe}_N$

A. Vega and L. C. Balbás

*Departamento de Física Teórica, Universidad de Valladolid, E-47011 Valladolid, Spain*

J. Dorantes-Dávila

*Instituto de Física "Manuel Sandoval Vallarta," Universidad Autónoma de San Luis Potosí,  
78000 San Luis Potosí, Mexico*

G. M. Pastor\*

*Institut für Theoretische Physik der Universität zu Köln,  
Zùlpicher Strasse 77, W-50937 Köln, Germany*

(Received 2 December 1993)

We present a study of the magnetic and electronic properties of  $\text{Fe}_N$  clusters embedded in antiferromagnetic bcc Cr. The spin-polarized charge distribution is determined self-consistently by solving a realistic *spd*-band model Hamiltonian including intra-atomic Coulomb interactions in the unrestricted Hartree-Fock approximation. For all the studied clusters ( $N \leq 51$ ), the local magnetic moments at Fe atoms close to the Fe-Cr interface, as well as the average magnetic moment of the  $\text{Fe}_N$  impurity, are reduced with respect to the Fe bulk magnetization. The magnetic order within  $\text{Fe}_N$  changes from antiferromagneticlike to ferromagneticlike with increasing cluster size. The calculated critical size for this transition is  $N_c \simeq 6$ . Results for the spatial distribution of the magnetic moments and for the local electronic densities of states are given for different  $N$ . The role of the structural and chemical local environment of the atoms on the electronic and magnetic properties is discussed, and our results are compared with those found for Fe/Cr multilayers. Some of the implications of the present study for magnetic alloys and ferromagnetic clusters on surfaces are pointed out.

## I. INTRODUCTION

Atomic clusters have opened new prospects in the development of material science. Taking advantage of the characteristic behavior of small particles, one expects to be able to tailor new materials for specific technological purposes, for example, for catalysis or magnetic recording. Consequently, the research effort invested in the study of the properties of these systems has been considerably large.<sup>1</sup>

In the past years remarkable progress has been achieved in the study of free clusters, in particular since it is possible to perform experiments on size-selected beams.<sup>1</sup> Although there is a multitude of fundamental and practical reasons to study *free clusters*, it is also true that for most technological applications the properties of *embedded clusters* (e.g., clusters in a matrix or deposited on a surface) are even more relevant. Therefore, it is of considerable importance to extend our present knowledge on free clusters to the situation where these clusters are embedded in a macroscopic environment. Comparison between the behavior of free and embedded clusters would also contribute significantly to the characterization of the specific properties of these materials.

The magnetic behavior of *3d* transition metals and their compounds is a subject of great interest in this context. Indeed, a large body of experimental and theoretical work has already shown that the magnetic properties

of itinerant *3d* electrons are very sensitive to the chemical and structural environment of the atoms. For example, the magnetic order in  $\text{Cr}_x\text{Fe}_{1-x}$  alloys changes from antiferromagnetic to ferromagnetic if the Fe concentration is increased beyond 20%. Moreover, for small  $x$  the average magnetization decreases approximately linearly with increasing  $x$ , and short-range-order effects due to clustering can strongly affect the magnetic and structural properties of these compounds.<sup>2</sup>

This kind of behavior has recently motivated the production and experimental study of a large variety of complex magnetic materials involving transition and noble metals in different geometrical arrangements such as overlayers, sandwiches, and multilayers.<sup>3,4</sup> In the particular case of the Fe/Cr system, one observes experimentally that the interlayer coupling of Fe films across a Cr film oscillates as a function of the Cr-spacer thickness  $d_{\text{Cr}}$  with a period of about 20 Å. For values of  $d_{\text{Cr}}$  yielding antiferromagnetic coupling between the Fe slabs, a giant magnetoresistance is observed which could be very useful for technological applications.<sup>4</sup> The Fe/Cr multilayers have been also the subject of extensive theoretical studies.<sup>5</sup> One observes that the magnetic order within the Fe and Cr slabs is qualitatively the same as in the corresponding pure solids and that the coupling at the interfaces is usually antiferromagnetic. A strong environment dependence of the local magnetic moments is found: The Fe moments at the interface are reduced with respect

to the bulk value, while in the middle of the slab they are sometimes enhanced. The Cr moments are not only modified close to the interface, but they are extremely sensitive to the compatibility of their spin density wave (SDW) state and the antiferromagnetic coupling at the Fe/Cr interfaces.<sup>5</sup>

In this paper we investigate the magnetic and electronic properties of bcc Fe<sub>N</sub> clusters with  $N \leq 51$  embedded in antiferromagnetic bcc Cr. This specific problem has been chosen not only for its potential technological relevance, but also since the magnetic properties of Fe and Cr are known to be very sensitive to the structural and chemical environment of the atoms. The competition between the tendency of the Fe clusters to order ferromagnetically<sup>6-10</sup> and the antiferromagnetism of the surrounding Cr matrix offers a particularly interesting physical situation for studying the interplay between the magnetic properties of the clusters and those of the environment. Moreover, from the perspective of the problem of Fe/Cr multilayers, this work provides a complementary study which stresses the local aspect of the magnetic interactions between Fe and Cr putting aside any translational symmetry or extended interfaces.

The rest of the paper is organized as follows. In the next section, a brief account of the theoretical method is given. Further details and applications to free clusters and surfaces can be found in Refs. 10-12. The results for bcc Fe<sub>N</sub> clusters in Cr are presented and discussed in Sec. III. We conclude in Sec. IV with a summary and by pointing out some of the implications of the present study for magnetic alloys and ferromagnetic clusters deposited on surfaces.

## II. THEORY

The magnetic properties at  $T = 0$  are determined by solving a realistic *spd*-band model Hamiltonian including intra-atomic Coulomb interactions in the unrestricted Hartree-Fock approximation. In the usual notation it is given by

$$H = \sum_{i\alpha\sigma} \varepsilon_{i\alpha\sigma} \hat{n}_{i\alpha\sigma} + \sum_{\substack{\alpha,\beta,\sigma \\ i \neq j}} t_{ij}^{\alpha\beta} \hat{c}_{i\alpha\sigma}^\dagger \hat{c}_{j\beta\sigma}, \quad (1)$$

where  $t_{ij}^{\alpha\beta}$  refer to the hopping integrals between sites  $i$  and  $j$  and orbitals  $\alpha$  and  $\beta$  ( $\alpha, \beta \equiv s, p, d$ ), and the spin-dependent energy levels are

$$\varepsilon_{i\alpha\sigma} = \varepsilon_{i\alpha}^0 + \sum_{\beta\sigma'} U_{\alpha\beta}^{\sigma\sigma'} \Delta\nu_{i\beta\sigma'} + z_i \Omega_\alpha. \quad (2)$$

In Eq. (2),  $\varepsilon_{i\alpha}^0$  stand for the orbital energy levels of the element at site  $i$  (e.g., Fe- or Cr) in the paramagnetic solution of the bulk. The second term takes into account the level shifts due to the redistribution of the spin-polarized density and the resulting intra-atomic Coulomb interactions.  $\Delta\nu_{i\beta\sigma} = \nu_{i\beta\sigma} - \nu_{i\beta\sigma}^0$ , where  $\nu_{i\beta\sigma} = \langle \hat{n}_{i\beta\sigma} \rangle$ , is the average electronic occupation of the spin orbital  $i\beta\sigma$ , and  $\nu_{i\beta\sigma}^0$  the corresponding average occupation in the paramagnetic solution of the bulk. The intra-atomic Coulomb integrals  $U_{\alpha\beta}^{\sigma\sigma'}$  can

be written in terms of the exchange and direct integrals  $J_{\alpha\beta} = U_{\alpha\beta}^{\uparrow\downarrow} - U_{\alpha\beta}^{\uparrow\uparrow}$  and  $U_{\alpha\beta} = (U_{\alpha\beta}^{\uparrow\downarrow} + U_{\alpha\beta}^{\uparrow\uparrow})/2$ . Finally, the last term in Eq. (2) takes into account the environment-dependent energy-level shifts due to nonorthogonality effects<sup>11,13</sup> (overlap interactions) and to the crystal-field potential of the neighboring atoms,<sup>14</sup> which are approximately proportional to the local coordination number  $z_i$ .

The number of electrons

$$\nu_\alpha(i) = \langle \hat{n}_{i\alpha\uparrow} \rangle + \langle \hat{n}_{i\alpha\downarrow} \rangle \quad (3)$$

and the local magnetic moments

$$\mu_\alpha(i) = \langle \hat{n}_{i\alpha\uparrow} \rangle - \langle \hat{n}_{i\alpha\downarrow} \rangle \quad (4)$$

at site  $i$  and orbital  $\alpha$  are determined self-consistently by requiring

$$\langle \hat{n}_{i\alpha\sigma} \rangle = \int_{-\infty}^{\varepsilon_F} \rho_{i\alpha\sigma}(\varepsilon) d\varepsilon. \quad (5)$$

The local density of states (DOS)  $\rho_{i\alpha\sigma}(\varepsilon) = (-1/\pi)\text{Im}\{G_{i\alpha\sigma, i\alpha\sigma}(\varepsilon)\}$  is determined by calculating the local Green's functions  $G_{i\alpha\sigma, i\alpha\sigma}(\varepsilon)$  by means of the recursion method.<sup>15</sup> The number of levels  $M$  of the continued fraction expansion of  $G_{i\alpha\sigma, i\alpha\sigma}$  is chosen large enough so that the physical results become independent of  $M$ .<sup>10</sup> For a single cluster impurity, the Fermi energy  $\varepsilon_F$  is that of the embedding matrix (in the present case Cr). Notice that spin-charge transfer between atoms and orbitals having different local environments may occur.

## III. RESULTS AND DISCUSSION

The parameters used in the calculations are determined as follows. The hopping integrals  $t_{ij}^{\alpha\beta}$  between atoms of the same element are fitted to band-structure calculations for the pure elements.<sup>16,17</sup> The heteronuclear hoppings at the cluster-matrix interface are obtained as the average of the corresponding homonuclear hoppings. This has been proved to be a very good approximation in calculations for alloy and multilayers of transition metals.<sup>5,16</sup> For simplicity we neglect the differences between  $s$  and  $p$  Coulomb integrals (i.e.,  $U_{ss} = U_{sp} = U_{pp}$  and  $U_{sd} = U_{pd}$ ) and take the ratios between the direct Coulomb integrals  $U_{ss} : U_{sd} : U_{dd}$  and  $U_{dd}(\text{Cr}) : U_{dd}(\text{Fe})$  from atomic Hartree-Fock calculations.<sup>18</sup> The absolute value of  $U_{dd}(\text{Fe}) = 5.40$  eV is estimated as the energy level shift which results when one  $d$  electron is transferred from an Fe atom to a nearest neighbor (NN).<sup>9</sup> The  $d$ -electron exchange integrals  $J_{dd}(\text{Fe}) = 1.06$  eV and  $J_{dd}(\text{Cr}) = 0.90$  eV yield the proper bulk magnetic moments [ $\mu(\text{Fe}) = 2.21\mu_B$  and  $\mu(\text{Cr}) = 0.60\mu_B$ ]. Exchange integrals other than  $J_{dd}$  are neglected. The orbital dependent constants  $\Omega_\alpha$  are given as the difference between the bare energy levels (i.e., excluding Coulomb shifts) of the isolated atom and the bulk. In this way we obtain, for Fe,  $\Omega_s = 0.312$  eV,  $\Omega_p = 0.484$  eV, and  $\Omega_d = -0.099$  eV, and for Cr,  $\Omega_s = 0.386$  eV,  $\Omega_p = 0.548$  eV, and  $\Omega_d = -0.171$  eV.<sup>19</sup>

The embedded Fe<sub>N</sub> clusters are located as substitutional impurities in the Cr bcc lattice. Small strain ef-

fects resulting from the minor differences in the lattice constants of Fe and Cr are modeled by taking the NN distance at the cluster-matrix interface as the average between the NN distances of the pure elements. The lattice structure around the  $\text{Fe}_N$  impurities are illustrated in Fig. 1. Here the numbers label the different nonequivalent atomic sites  $i$  at which the spin-dependent electronic charge distribution has been calculated self-consistently. The charge distributions at matrix atoms located farther than the third NN from the interface are taken to be the same as in pure Cr. This can be considered to be a good approximation as long as the magnetic moments and charge distribution obtained for the third Cr nearest neighbor of the  $\text{Fe}_N$  cluster are already close to the pure Cr value (see Table I and the discussion below). For  $\text{Fe}_N$  with  $N = 1, 9, 15, 27,$  and  $51$  the atoms of different symmetry belong to the different NN shells of the bcc lattice. The cubic local symmetry is preserved after the Cr atoms are replaced by the Fe atoms (see Fig. 1). This is not the case for the  $\text{Fe}_2, \text{Fe}_4$  (tetrahedron), and  $\text{Fe}_6$  (bipyramid) impurities. In these cases the spin-polarized charge distribution must be computed at a larger number of nonequivalent sites.

Results for the local magnetic moments  $\mu(i)$  of embedded  $\text{Fe}_N$  clusters with  $N \leq 51$  are given in Table I. In Figs. 2 and 3 the  $\mu(i)$  are plotted as a function of  $i$ . The sites  $i$  are labeled in order of increasing distance to the center of the cluster. Thus, the spatial distribution of the local magnetic moments and the convergence to the corresponding periodic crystals can be directly inferred.

Before discussing the results for small  $\text{Fe}_N$  clusters, we consider the case of an atomic impurity ( $N = 1$ ). For a single Fe atom embedded in the antiferromagnetic Cr matrix, we obtain a very small charge transfer between the different symmetry atoms. The calculated  $s, p,$  and  $d$  orbital occupations are very similar to those of the corresponding bulk atoms. However, the spin polarizations

are very different. The smaller exchange splitting at the Cr atoms surrounding the Fe impurity and the antiferromagnetic order in the matrix lead to a strong reduction of the spin polarization at the Fe atom. The local magnetic moment of the Fe impurity couples antiferromagnetically with the Cr NN. This is compatible with the spin density wave (SDW) of the Cr matrix [see Table I and Fig. 2(a)]. The same trend is also observed at the interface of larger embedded clusters, as will be discussed in more detail below. The small calculated magnetic moment at the Fe impurity contrasts with the known large value of pure bulk Fe. The importance of the cluster-matrix interactions to the magnetic properties of the system is evident.

Interesting trends are observed as the size of the cluster impurity is increased. For very small cluster sizes, the hybridization of the Fe and Cr orbitals cause the largest effects on the properties of the Fe clusters and lead to remarkable qualitative changes in their magnetic behavior. In fact,  $\text{Fe}_2$  and  $\text{Fe}_4$  order *antiferromagnetically* and the local magnetic moments are strongly reduced as compared to free  $\text{Fe}_N$  or Fe bulk.<sup>8-10</sup> In these cases the magnetic order at the interface and within the Fe cluster is the same as in pure Cr (see Table I). In other words, very small Fe clusters in Cr adopt the short-range magnetic order prescribed by the SDW of the matrix. The calculated absolute values of the  $\mu(i)$  in  $\text{Fe}_N$  are almost the same for  $N = 1, 2,$  and  $4$ . The reduction of  $|\mu(i)|$  at Fe atoms can be qualitatively understood by recalling that almost all the neighbors of the Fe atoms are Cr atoms which have a much smaller exchange splitting than the Fe atoms in  $\alpha\text{-Fe}$ . Similar trends are also observed at the interface of larger  $\text{Fe}_N$  clusters in Cr, as well as at the interfaces of Fe/Cr overlayers and multilayers.<sup>3-5</sup>

The expected transition to more  $\alpha\text{-Fe}$ -like properties within the  $\text{Fe}_N$  impurity starts to set in for somewhat larger clusters.  $\text{Fe}_6$  in Cr already shows ferromagneticlike order (i.e., all local moments pointing in the

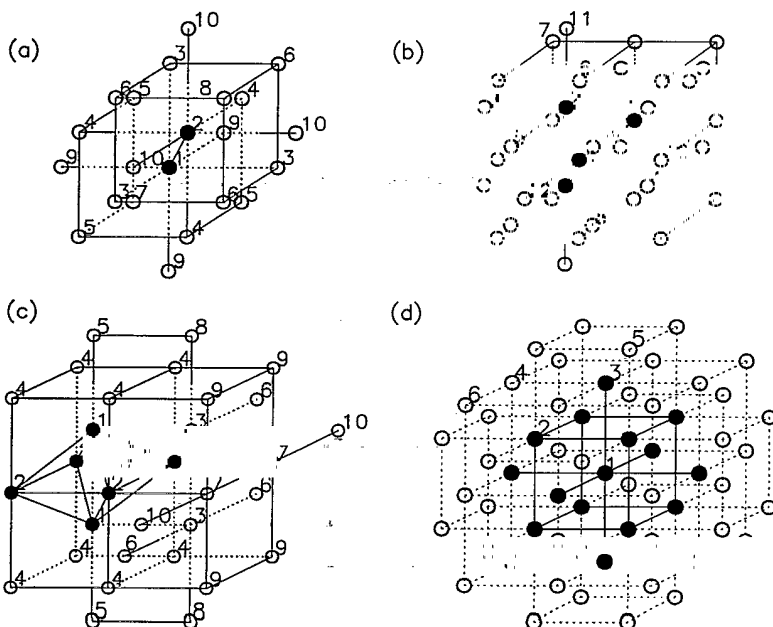


FIG. 1. Illustration of the lattice structure around  $\text{Fe}_N$  clusters embedded in bcc Cr as substitutional impurities: (a)  $\text{Fe}_2$ , (b)  $\text{Fe}_4$ , (c)  $\text{Fe}_6$ , and (d)  $\text{Fe}_{15}$ . The Fe (Cr) atoms are represented with solid (open) circles. The numbers label the different nonequivalent atomic sites  $i$ , taking into account the chemical composition and spin polarizations. For  $N = 1, 9, 27,$  and  $51$  the labels  $i$  correspond to the successive nearest neighbor shells in the bcc lattice as for  $\text{Fe}_{15}$ .

TABLE I. Local magnetic moments  $\mu(i)$  (in units of  $\mu_B$ ) for bcc  $\text{Fe}_N$  clusters embedded in Cr. The lattice structure around  $\text{Fe}_N$  and the labels  $i$  for the different atomic sites are shown in Fig. 1. The distance of the atoms to the center of the cluster increases (nonstrictly) with  $i$ . The chemical composition of each lattice site (Fe or Cr) is indicated together with the sign (in brackets) that the magnetization would have at this site in pure antiferromagnetic Cr.

$i$ $N$	1	2	3	4	5	6	7	8	9	10	11	12
1	0.26 Fe(+)	-0.61 Cr(-)	0.61 Cr(+)	0.60 Cr(+)								
2	0.26 Fe(+)	-0.26 Fe(-)	0.61 Cr(+)	-0.61 Cr(-)	-0.61 Cr(-)	0.61 Cr(+)	-0.60 Cr(-)	0.60 Cr(+)	0.60 Cr(+)	-0.60 Cr(-)		
4	0.26 Fe(+)	-0.26 Fe(-)	0.62 Cr(+)	-0.62 Cr(-)	-0.61 Cr(-)	0.61 Cr(+)	0.60 Cr(+)	-0.60 Cr(-)	-0.61 Cr(-)	0.61 Cr(+)	-0.60 Cr(-)	0.60 Cr(+)
6	1.20 Fe(-)	0.78 Fe(+)	-0.60 Cr(-)	0.54 Cr(+)	-0.58 Cr(-)	-0.60 Cr(-)	0.58 Cr(+)	-0.59 Cr(-)	0.58 Cr(+)	0.60 Cr(+)		
9	2.24 Fe(-)	0.61 Fe(+)	-0.65 Cr(-)	-0.62 Cr(-)	0.59 Cr(+)							
15	2.21 Fe(+)	1.42 Fe(-)	1.59 Fe(+)	0.39 Cr(+)	-0.60 Cr(-)	0.49 Cr(+)						
27	2.23 Fe(+)	2.18 Fe(-)	1.57 Fe(+)	0.99 Fe(+)	-0.75 Cr(-)	0.53 Cr(+)	0.59 Cr(+)					
51	2.42 Fe(-)	2.14 Fe(+)	2.31 Fe(-)	1.97 Fe(-)	1.29 Fe(+)	-0.89 Cr(-)	-0.88 Cr(-)	0.50 Cr(+)				

same direction). The local magnetic moments in  $\text{Fe}_8$  are appreciably larger than in the smaller antiferromagnetic cluster impurities ( $N \leq 4$ ), although they are still far from the Fe-bulk value (see Table I). Larger  $\text{Fe}_N$  clusters in Cr also show ferromagneticlike order. A transition from antiferromagnetic to ferromagnetic order within  $\text{Fe}_N$  is thus found at the critical cluster size  $N_c = 6$  (see Figs. 2 and 3).

The Cr atoms close to the  $\text{Fe}_N$  cluster preserve the antiferromagnetic order given by the rest of the Cr matrix; i.e., the  $\mu(i)$  do not change sign upon introducing the  $\text{Fe}_N$  impurity (see Table I). As pointed out before,  $\text{Fe}_N$  clusters in Cr show ferromagneticlike order for  $N \geq N_c = 6$ . The magnetic coupling at the cluster-matrix interface is mainly antiferromagnetic. This is qualitatively in agreement with experiments and theoretical calculations on Fe/Cr overlayers and multilayers, and reflects the tendency of bcc Fe towards ferromagnetism and of bcc Cr towards antiferromagnetism.<sup>3-5</sup> However, notice that the details of the magnetic order at the interface depend very much on the structure of the cluster and the matrix. For example, for  $\text{Fe}_{15}$  and  $\text{Fe}_{51}$  it is not possible to preserve the ferromagnetic order within the cluster and at the same time a perfect antiferromagnetic coupling between all Fe-Cr and Cr-Cr NN. The reason is that the atoms at the interface do not belong to a single magnetic sublattice, as can be seen for  $\text{Fe}_{15}$  at the atoms labeled 2, 3, and 4 in Fig. 1(d). This magnetic mismatch, which is not present in  $\text{Fe}_9$  and  $\text{Fe}_{27}$ , possibly contributes to the reduction of the spin polarization at these sites, as well

as to the oscillations of  $|\mu(i)|$  within the Fe clusters and at Cr atoms close to the interface. Similar strong perturbations on the spatial distribution of the local moments have been found in Fe/Cr (001) multilayers, when magnetic frustrations are present due to interface roughness or because the magnetic arrangement of the Fe slabs is incompatible with the SDW of Cr.<sup>5</sup>

The local magnetic moments at the Fe atoms decrease as we go from the center of the Fe cluster to the Fe-Cr interface and are reduced with respect to the Fe-bulk magnetization (see Figs. 2 and 3). This contrasts with the behavior of free Fe clusters where, as a consequence of the reduction of the local coordination number, an increase of the local magnetic moments is found at the cluster surface.<sup>8-10</sup> The decrease of  $\mu(i)$  at Fe atoms close to the interface can be related to the local environment of these atoms and in particular to the chemical composition of its first NN shell. From the results shown in Table I one sees that the  $\mu(i)$  at Fe atoms increase nearly monotonically with the number of Fe atoms  $\xi_i$  which are the first NN's of  $i$ . For example, in  $\text{Fe}_{15}$   $\xi_2 = \xi_3 = 4$  and  $\mu(2) = 1.42\mu_B$ ,  $\mu(3) = 1.59\mu_B$ ; in  $\text{Fe}_{27}$   $\xi_3 = 4$  and  $\mu(3) = 1.57\mu_B$ . In  $\text{Fe}_{51}$   $\xi_5 = 3$  and  $\mu(5) = 1.29\mu_B$ . In  $\text{Fe}_{27}$   $\xi_4 = 2$  and  $\mu(4) = 0.99\mu_B$ . Finally, in  $\text{Fe}_9$   $\xi_2 = 1$  and  $\mu(2) = 0.61\mu_B$ . The same trend also holds for smaller clusters (e.g., for  $\text{Fe}_8$ ), where all Fe atoms are at the interface. In agreement with this picture we find that  $\mu(i)$  is close to the Fe-bulk value  $\mu_b(\text{Fe}) = 2.21\mu_B$  as soon as all first NN's of an Fe atom are also Fe. Nevertheless, such a fast convergence to  $\mu_b$  is somewhat surprising since  $\mu(i)$  and

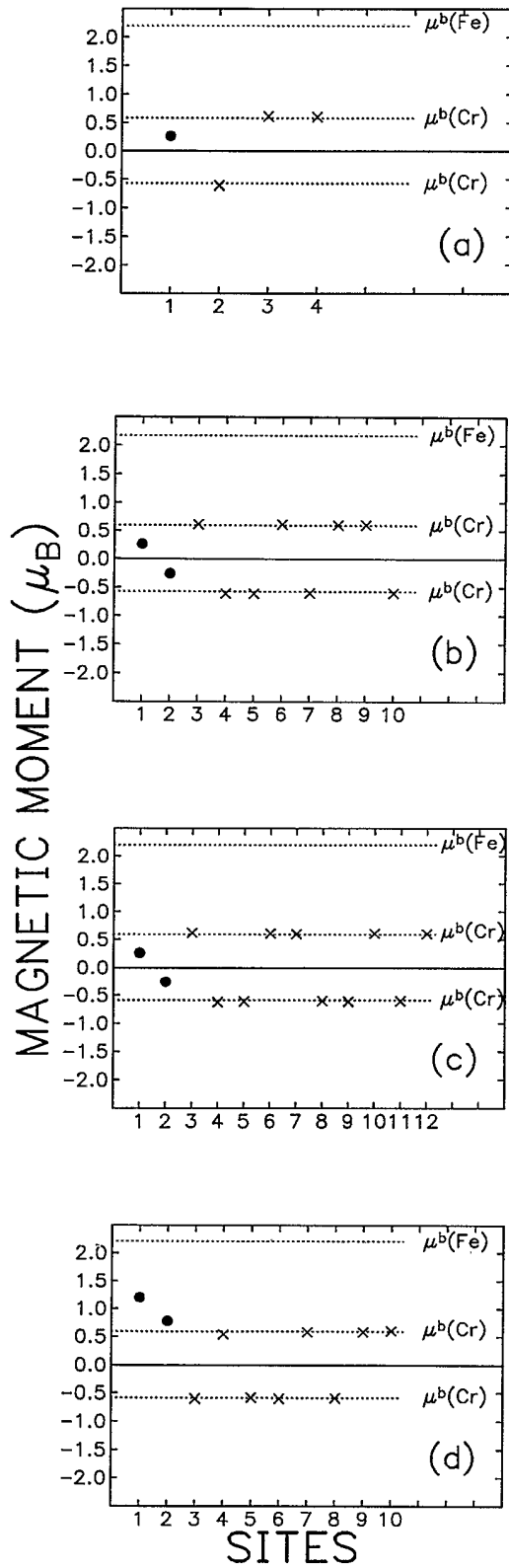


FIG. 2. Spatial distribution of the local magnetic moments  $\mu(i)$  for  $\text{Fe}_N$  clusters embedded in Cr: (a)  $\text{Fe}_1$ , (b)  $\text{Fe}_2$ , (c)  $\text{Fe}_4$ , and (d)  $\text{Fe}_6$ . The nonequivalent atomic sites  $i$  are ordered by increasing distance to the center of the cluster, as indicated in Fig. 1. Dots (crosses) correspond to Fe (Cr) atoms. Notice the transition from antiferromagnetic to ferromagnetic order with increasing  $N$ .

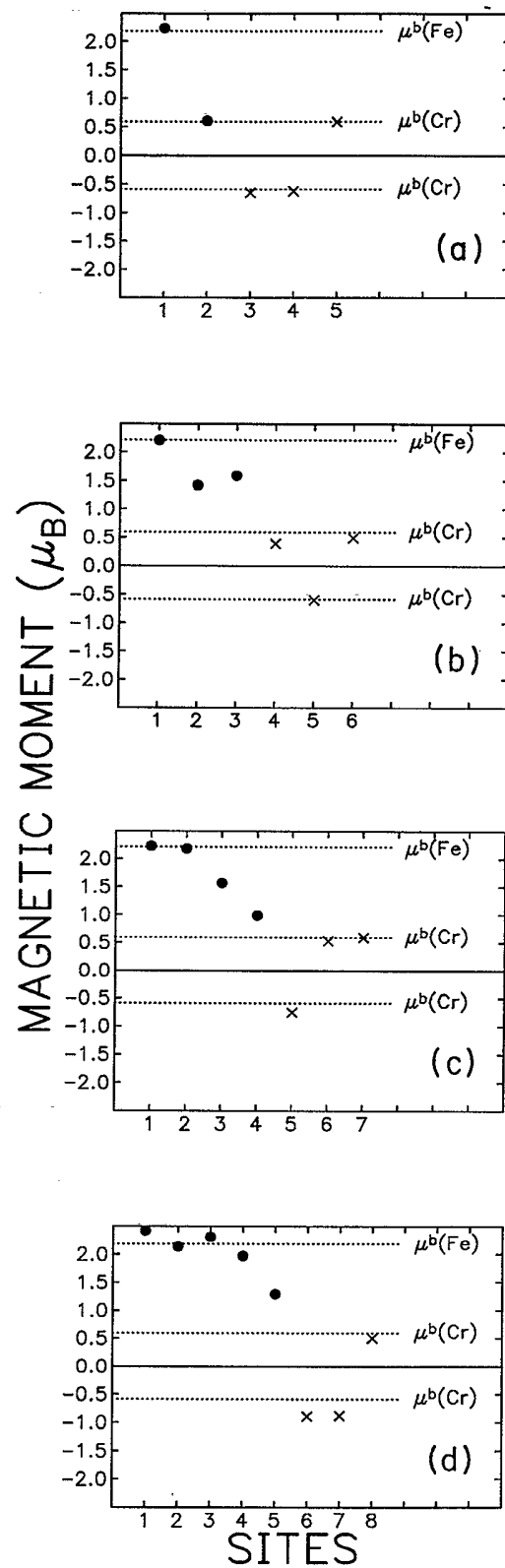


FIG. 3. Spatial distribution of the local magnetic moments  $\mu(i)$  for  $\text{Fe}_N$  clusters embedded in Cr: (a)  $\text{Fe}_9$ , (b)  $\text{Fe}_{15}$ , (c)  $\text{Fe}_{27}$ , and (d)  $\text{Fe}_{51}$ . The nonequivalent atomic sites  $i$  are ordered by increasing distance to the center of the cluster, as indicated in Fig. 1. Dots (crosses) correspond to Fe (Cr) atoms. Notice the decrease of the  $\mu(i)$  of the Fe atoms at the Fe-Cr interface.

the 3d exchange splitting at the neighboring Fe atoms is much smaller than in pure Fe (see, for instance,  $N = 9$  or  $N = 15$  in Table I). Notice that for Fe<sub>51</sub> in Cr some of the  $\mu(i)$  at Fe atoms are larger than  $\mu_b$ , although the average magnetization per Fe atom is always smaller than  $\mu_b$ . A similar behavior has been found in Fe/Cr multilayers, where the  $\mu(i)$  at the center of an Fe slab can be enhanced with respect to the Fe-bulk magnetization.<sup>5</sup> It should also be observed that for  $N = 15$  and  $N = 51$  our results for  $\mu(i)$  could slightly change ( $\approx 0.1\mu_B$ ) if we include farther Cr sites in the self-consistent calculations, since the  $\mu(i)$  at the outermost Cr atoms, where the charge distribution is computed self-consistently, are not very close to the Cr-bulk magnetic moment  $\mu_b(\text{Cr}) = 0.6\mu_B$  (see Table I). Moreover, in the presence of frustrations one should also consider the possibility that the system develops, close to the embedded cluster, a more complex magnetic structure with noncollinear spins. In fact, noncollinear spin arrangements can be shown to lower considerably the energy of free clusters with nonbipartite structures for some band fillings.<sup>20</sup> In the present case, however, the SDW state of the Cr matrix sets a boundary condition which should tend to reduce the stability of such spin arrangements.

Our results show that Fe<sub>N</sub> clusters embedded in Cr have many features in common with the Fe/Cr multilayers: The ferromagnetic order obtained in Fe<sub>N</sub> for not too small  $N$ , the antiferromagnetic order in the Cr matrix (even close to the interface with the ferromagnet), the antiferromagnetic coupling at the Fe/Cr interface, the strong reduction of the Fe local moments close to the interface, the possibility of enhancement of  $\mu(i)$  at the center of an Fe cluster or slab, and the strong perturbation of the magnetic moments at both Fe and Cr atoms due to frustrations are all characteristic properties which both finite-cluster and extended-layered Fe-Cr systems share. One concludes that, at least in this case, the immediate local environment of the atoms gives the main contribution to the magnetic behavior, although for quantitative predictions, the details of the electronic structure, and thus the geometrical arrangement at a larger length scale, are also important.

Concerning the redistribution of the electronic charge, it is worth noting that for all studied Fe clusters in Cr, the calculated interatomic charge transfer between nonequivalent sites is very small (typically  $|\Delta\nu_i| < 0.05$ ). This is consistent with the approximation of local charge neutrality often used in surface calculations.<sup>16,21</sup> Our approximation for the variations of the crystal-field potential and overlap interactions with the local environment yields properly this physically expected behavior. The small values of  $|\Delta\nu_i|$  also justify *a posteriori* the fact that the interatomic Coulomb interactions  $U_{ij}$  are not taken explicitly into account in our self-consistent calculations.<sup>22</sup> The same model has been applied successfully to free clusters and semi-infinite systems, where the reduction of the local coordination number  $z_i$  at the surface leads to a larger correction of the energy levels than in the present case.<sup>10,12,14</sup> Here all atoms have the same  $z_i$  and the level shift is due to their different chemical environment. The magnetic properties such as local

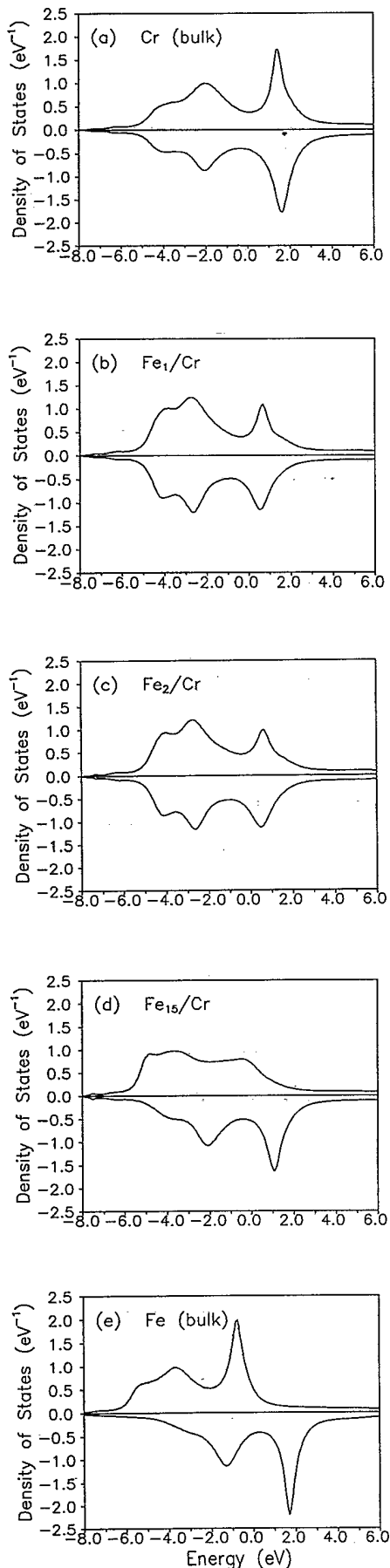
magnetic moments and magnetic order are not significantly affected by the small  $sp$ - and  $d$ -charge redistributions we obtain ( $|\Delta\nu_{sp}| \approx 0.02$  and  $|\Delta\nu_d| \approx 0.05$ ). Nonetheless, some interesting trends can be pointed out. For example, at the embedded Fe cluster the number of  $sp$  electrons usually increases somewhat, whereas the Cr atoms at the interface show in most cases a decrease of the electron density mainly of  $d$  electrons. A rapid convergence to the Cr-bulk charge distribution is reached as soon as most of the first and second NN's are also Cr atoms.

Detailed information about the hybridization between the electronic states of the Fe<sub>N</sub> impurity and the Cr matrix can be inferred from the local densities of electronic states (DOS). In Fig. 4 the DOS of a few representative Fe<sub>N</sub> clusters embedded in Cr are shown. The DOS of pure Cr and Fe are also given for sake of comparison. The results for Fe<sub>1</sub> and Fe<sub>2</sub> show a remarkable resemblance to the DOS of Cr. The valley around the Fermi energy and the structure in the up and down DOS are typical of antiferromagnetic Cr. In Fe<sub>1</sub> and Fe<sub>2</sub>, the up and down DOS are quantitatively very similar, which results in very small local magnetic moments, yet smaller than in pure Cr. A clearly different behavior is found for larger clusters as Fe<sub>15</sub>. The Fermi energy lies now above the main antibonding peak in the up (majority) DOS and below the main antibonding peak in the down DOS, as in pure Fe. The exchange splitting is markedly larger than in Fe<sub>1</sub> or Fe<sub>2</sub> and the shift between the up and down DOS has much of a ferromagnetic character. However, the changes in the DOS due to the hybridization with the Cr matrix are still appreciable, particularly in the up DOS.<sup>23</sup> Varying the cluster-impurity size from Fe<sub>2</sub> to Fe<sub>15</sub> we also observe the changes in the electronic structure due to the transition from antiferromagnetic to ferromagnetic order within Fe<sub>N</sub>. Photoemission experiments on these systems would be of considerable interest.

#### IV. SUMMARY AND OUTLOOK

The magnetic and electronic properties of bcc clusters embedded in Cr as a single substitutional impurity have been investigated by solving a realistic  $spd$ -band model Hamiltonian in the unrestricted Hartree-Fock approximation. The changes in the spin-polarized charge distribution and in the local densities of states (DOS) which result from the particular local environment of the Fe and Cr atoms have been calculated self-consistently for  $N \leq 51$ . The main conclusions of this study are summarized below.

(i) Small Fe<sub>N</sub> clusters in Cr order antiferromagnetically as the Cr matrix for  $N \leq 4$ . For larger Fe<sub>N</sub> ( $N \geq 6$ ) the magnetic order within the Fe cluster is ferromagnetic-like, while the magnetic coupling at Fe-Cr interface remains antiferromagnetic, as far as the structure of the interface allows it. As a result of the cluster-matrix interactions, a transition from antiferromagnetic to ferromagnetic order occurs within the embedded Fe<sub>N</sub> cluster at the critical size  $N_c \simeq 6$ . For the studied clusters ( $N \leq 51$ ) the local magnetic order at Cr atoms close



to the interface is not altered by the presence of the Fe atoms.

(ii) The magnetic moments  $\mu(i)$  are very sensitive to the local environment of atom  $i$ . At Fe atoms close to the Fe-Cr interface  $\mu(i)$  is strongly reduced with respect to the Fe-bulk magnetization  $\mu_b$ . This can be qualitatively related to the chemical composition of the first NN's shell of  $i$ . For Fe atoms,  $\mu(i)$  increases with increasing number of Fe atoms in the NN shell of  $i$  and reaches values close to  $\mu_b$  (in some cases even larger than  $\mu_b$ ) when all NN's are Fe.

(iii) The local electronic densities of states (DOS) of the embedded  $\text{Fe}_N$  cluster reflect very clearly the size-dependent change of the magnetic order and the proximity effects. For instance, the DOS of  $\text{Fe}_2$  is typically antiferromagnetic and looks very similar to that of bulk Cr, while the DOS of  $\text{Fe}_{15}$  shows a ferromagnetic exchange splitting and the main features of the DOS of bulk Fe start to be present.

(iv) In spite of the strong environment dependence of the local magnetic moments and electronic DOS, the calculated intra-atomic and interatomic *spd*-charge transfers result in being very small and having no significant influence on the magnetic properties. This gives additional support to the approximations of local charge neutrality and neglect of intra-atomic *sp-d* charge transfer often used in surface and alloy calculations.<sup>16,21</sup>

(v) The magnetic properties of not too small  $\text{Fe}_N$  clusters embedded in Cr are very similar to those of Fe/Cr sandwiches and multilayers. This indicates that the extended character of an interface is qualitatively not so important for properties like the distribution of the local moments  $\mu(i)$  or the magnetic coupling at the interface, and that the immediate neighborhood of the atoms gives the dominant contribution.

These trends show once more the importance of the cluster-matrix interactions to the magnetic properties of itinerant electrons. For  $\text{Cr}_x\text{Fe}_{1-x}$  alloys, this implies that cluster formation due to the alloying process or segregation can considerably change the magnetic behavior of materials of given concentrations. Our work could be extended to study the interaction among clusters in a matrix in order to obtain quantitative information about this problem. Other embedding matrices should also be considered. In particular for nonmagnetic metals one would like to know which is the smallest  $N$  for which  $\text{Fe}_N$  impurities are magnetic and how the magnetic moments depend on  $N$  and on the characteristics of the matrix. This could be relevant for the development of dense magnetic recording media.

It has been shown that the magnetic properties of  $\text{Fe}_N$

FIG. 4. Local electronic density of states (DOS) of  $\text{Fe}_N$  clusters embedded in Cr as a function of the energy relative to the Fermi energy. Positive (negative) values refer to up (down) spin. For antiferromagnetic  $\text{Fe}_2$  the DOS at one of the Fe atoms is given and for ferromagnetic  $\text{Fe}_{15}$  the cluster-average DOS is shown. The results for pure Cr and Fe are also given for sake of comparison. Notice how the electronic spectrum reflects the changes in the local magnetic order and proximity effects.

clusters in Cr are qualitatively different from those of free (nonembedded) clusters in some important respects. While in free clusters the local magnetic moments  $\mu(i)$  and the magnetization per atom are larger than in Fe bulk, the embedded clusters studied here show the opposite behavior. Now, for Fe clusters deposited on antiferromagnetic or nonmagnetic surfaces, both cluster-substrate interactions and reductions of the local coordination number are present. As a result of these competing effects, a variety of interesting magnetic phenomena can be expected. Moreover, the magnetic and electronic

properties of finite clusters or islands deposited on surfaces are of great technological interest. Further theoretical work in this direction is worthwhile.

#### ACKNOWLEDGMENTS

This work has been supported by DGICYT (Spain), Junta de Castilla y León (Spain), Acciones Integradas Hispano-Alemanas, the Deutsche Forschungsgemeinschaft (SFB 341), and CONACyT (Mexico) through Grant No. 0932-E9111.

\*Present address: Departamento de Física de la Materia Condensada, Facultad de Ciencias, Universidad Autónoma de Madrid, E-28049 Madrid, Spain.

<sup>1</sup>*Proceedings of the VIth International Symposium on Small Particles and Inorganic Clusters*, Chicago, September 1992 [*Z. Phys. D* **26** (1993)]; *Proceedings of the First International Conference on Nanostructured Materials*, Cancún (México), September 1992 [*Nanostruct. Mater.* **6** (1993)].

<sup>2</sup>S.K. Burke and B.D. Rainford, *J. Phys. F* **13**, 441 (1983); **13**, 471 (1983); S.K. Burke, R. Cywinski, J.R. Davis, and B.D. Rainford, *ibid.* **13**, 451 (1983).

<sup>3</sup>J. Unguris, R.J. Celotta, and D.T. Pierce, *Phys. Rev. Lett.* **69**, 1125 (1992); T.G. Walker, A.W. Pang, H. Hopster, and S.F. Alvarado, *ibid.* **69**, 1121 (1992); F.U. Hillebrecht, Ch. Roth, R. Jungblut, E. Kisker, and A. Bringer, *Europhys. Lett.* **19**, 711 (1992); R.W. Wang, D.L. Mills, E.C. Fullerton, J.E. Mattson, and S.D. Bader, *Phys. Rev. Lett.* **72**, 920 (1994).

<sup>4</sup>P. Grünberg, R. Schreiber, Y. Pang, M.B. Brodsky, and H. Sowers, *Phys. Rev. Lett.* **57**, 2442 (1986); C. Carbone and S.F. Alvarado, *Phys. Rev. B* **36**, 2433 (1987); M.N. Baibich, J.M. Broto, A. Fert, F. Nguyen Van Dau, F. Petroff, P. Eitenne, G. Creuzet, A. Friederich, and J. Chazelas, *Phys. Rev. Lett.* **61**, 2472 (1988); J.J. Krebs, P. Lubitz, A. Chaiken, and G. Prinz, *ibid.* **63**, 4828 (1989); S.S.P. Parkin, N. More, and K.P. Roche, *ibid.* **64**, 2304 (1990); S. Demokritov, J.A. Wolf, and P. Grünberg, *Europhys. Lett.* **15**, 881 (1991).

<sup>5</sup>P.M. Levy, K. Ounadjela, S. Zhang, Y. Wang, C.B. Sommers, and A. Fert, *J. Appl. Phys.* **67**, 5914 (1990); F. Herman, J. Sticht, and M. van Schilfgaarde, *ibid.* **69**, 4783 (1991); K. Ounadjela, C.B. Sommers, A. Fert, D. Stoefler, F. Gautier, and V.L. Moruzzi, *Europhys. Lett.* **15**, 875 (1991); D. Stoefler and F. Gautier, *Phys. Rev. B* **44**, 10389 (1991); Z.-P. Shi, P.M. Levy, and J.L. Fry, *Phys. Rev. Lett.* **69**, 3678 (1992); J.-h. Xu and A.J. Freeman, *Phys. Rev. B* **47**, 165 (1993).

<sup>6</sup>W.A. de Heer, P. Milani, and A. Châtelain, *Phys. Rev. Lett.* **65**, 488 (1990); I.M.L. Billas, J.A. Becker, A. Châtelain, and W.A. de Heer, *ibid.* **71**, 4067 (1993).

<sup>7</sup>J.P. Bucher, D.G. Douglas, and L.A. Bloomfield, *Phys. Rev. Lett.* **66**, 3052 (1991); D.C. Douglass, A.J. Cox, J.P. Bucher, and L.A. Bloomfield, *Phys. Rev. B* **47**, 12874 (1993).

<sup>8</sup>K. Lee, J. Callaway, K. Kwong, R. Tang, and A. Ziegler,

*Phys. Rev. B* **31**, 1796 (1985), and references therein.

<sup>9</sup>G.M. Pastor, J. Dorantes-Dávila, and K.H. Bennemann, *Physica B* **149**, 22 (1988); *Phys. Rev. B* **40**, 7642 (1989); J. Dorantes-Dávila, H. Dreyssé, and G.M. Pastor, *ibid.* **46**, 10432 (1992).

<sup>10</sup>A. Vega, L.C. Balbás, J. Dorantes-Dávila, and G.M. Pastor, *Phys. Rev. B* **47**, 4742 (1993).

<sup>11</sup>J. Dorantes-Dávila, A. Vega, and G.M. Pastor, *Phys. Rev. B* **47**, 12995 (1993).

<sup>12</sup>A. Vega, L.C. Balbás, J. Dorantes-Dávila, and G.M. Pastor, *Surf. Sci.* **251/252**, 55 (1991).

<sup>13</sup>W.A. Harrison, *Electronic Structure and the Properties of Solids* (Freeman, San Francisco, 1980); M. van Schilfgaarde and W.A. Harrison, *Phys. Rev. B* **33**, 2653 (1986).

<sup>14</sup>G.M. Pastor, J. Dorantes-Dávila, and K.H. Bennemann, *Chem. Phys. Lett.* **148**, 459 (1988).

<sup>15</sup>R. Haydock, in *Solid State Physics*, edited by E. Ehrenreich, F. Seitz, and D. Turnbull (Academic, London 1980), Vol. 35, p. 215.

<sup>16</sup>R.H. Victora, L.M. Falicov, and S. Ishida, *Phys. Rev. B* **30**, 3896 (1984).

<sup>17</sup>D.A. Papaconstantopoulos, *Handbook of the Band Structure of Elemental Solids* (Plenum, New York, 1986).

<sup>18</sup>J.B. Mann, *Atomic Structure Calculations*, Los Alamos Sci. Lab. Rept. LA-3690, 1967.

<sup>19</sup> $\Omega_s, \Omega_p > 0$  indicates that the repulsive shift due to overlap interactions dominates for *sp* electrons. For the more localized *d* electrons  $\Omega_d$  is smaller and negative indicating that the attractive crystal-field shift is more important in this case.

<sup>20</sup>M.A. Ojeda, J. Dorantes-Dávila, and G.M. Pastor (unpublished).

<sup>21</sup>A. Vega, L.C. Balbás, H. Nait-Laziz, C. Demangeat, and H. Dreyssé, *Phys. Rev. B* **48**, 985 (1993); A. Vega, L.C. Balbás, and H. Dreyssé, *J. Magn. Magn. Mater.* **121**, 177 (1993).

<sup>22</sup>For other matrices (e.g., V) the charge transfer may be somewhat larger and interatomic Coulomb interactions may be necessary for a proper description of the screening of the induced charge density: A. Vega and G.M. Pastor (unpublished).

<sup>23</sup>The effects of the Cr matrix on the electronic structure of the Fe cluster are also evident by comparing the DOS of Fig. 4 with the corresponding results for free clusters given in Refs. 9 and 10.